

Fine structure of Rydberg states: $n = 6$ and 7 D and F states of ${}^4\text{He}^\dagger$

Keith B. MacAdam

Department of Physics, University of Arizona, Tucson, Arizona 85721

William H. Wing

Department of Physics and Optical Sciences Center, University of Arizona, Tucson, Arizona 85721

(Received 19 May 1975)

We have measured all the fine-structure intervals in the configurations $1s7d$ and $1s7f$ of ${}^4\text{He}$ as well as the intervals $6^1D_2-6^1F_3$ and $6^1D_2-6^3F_3$ by a microwave-optical-resonance method. The level of accuracy considerably exceeds that of available calculations. We discuss the results in relation to the breakdown of LS coupling, and we estimate the singlet-triplet mixing coefficients and the corresponding level perturbations. We obtain an improved fitting formula useful for predicting the frequencies of $n^1D_2-n^1,^3F_3$ transitions.

I. INTRODUCTION

The fine structure of helium has long been a testing ground for approximate solutions to the relativistic atomic three-body problem.¹⁻⁶ In addition, singlet-triplet splittings, which result from both electrostatic and relativistic effects, are of current interest because of their relation to the breakdown of Russell-Saunders LS coupling in helium.⁷⁻¹²

Experimentally, helium relativistic fine structure was first studied in optical spectra by Houston.¹³ The most accurate measurements have been made using microwave methods.^{14,15} Microwave transitions in high-lying singly excited states of the helium atom, involving both relativistic and electrostatic fine-structure intervals, were reported by Wing, Mader, and Lamb.^{16,17} Violations of various selection rules as a result of external perturbations were noted in states as high as $n=20$. In a subsequent precise experiment using the microwave-optical-resonance method^{18,19} in a field-free region, Wing and Lamb²⁰ measured the frequencies of the two relatively strong transitions between the states $1s7d^1D_2$ and $1s7f^1,^3F_3$ near 31 500 MHz ($1 \text{ MHz} = 3.34 \times 10^{-5} \text{ cm}^{-1}$) to an accuracy of ± 0.1 MHz. The results showed clearly that breakdown of LS coupling occurs in those $7F$ states having $J=L$.

In this article we present results of comparable accuracy for the complete set of microwave transitions between fine structure (fs) sublevels of the $1s7d$ and $1s7f$ configurations of ${}^4\text{He}$. In the present work the frequency range was extended to cover 44–52 GHz and signal-handling circuits were improved. The eight relatively weak transitions of the type $7^3D_J-7^1,^3F_J$, were found near 45 000 MHz. From the transition frequencies all the electrostatic and relativistic fs splittings in these configurations

were obtained with an accuracy of a few tenths of 1 MHz. The two transitions $6^1D_2-6^1,^3F_3$ near 49 800 MHz were also measured. From these the 200-MHz $6F$ singlet-triplet splitting was obtained with similar accuracy. The resonances were observed over a range of helium-pressure, microwave-power, and electron-bombardment conditions to check for shifts or broadening of the resonances. No significant shifts were observed in the $n=6$ data, but an effect of collisional excitation transfer in $n=7$ was observed, as described in Sec. V. A fitting formula²¹ is given for the $n^1D_2-n^1,^3F_3$ transition series. This formula may be useful in narrowing the search for other resonances in highly excited states of helium. Estimates are made of the singlet-triplet mixing coefficients in the $7D$, $6F$, and $7F$ states based on the results and on the Breit-Bethe analysis of helium fs.^{1,4}

Several nD fs measurements of lower precision have been reported by others for $n=3-8$. The spatial frequency of quantum beats in beam-foil experiments can be related to relativistic fs.²² Uncertainties from 2 to 30 MHz have been obtained in such experiments.²³ However, no beam-foil measurements of singlet-triplet differences have been reported. Results for 3^3D through 7^3D fine structures have been obtained from several level-crossing experiments.²⁴⁻²⁸ The uncertainties quoted are normally smaller than those in beam-foil work, ranging from a few tenths of 1 MHz to a few MHz. Aside from optical measurements,²⁹⁻³¹ only the anticrossing experiments of Miller *et al.*³² have obtained singlet-triplet D intervals. The uncertainties reported are 20–40 MHz for $n=6-8$.

Litzen³⁰ reported $n^1,^3F$ intervals in $n=4-6$ from optical measurements, but the level uncertainties were of the same order as the level separations ($0.005-0.010 \text{ cm}^{-1}$). The $5^3F_3-5^3F_4$ interval was measured in a level-crossing experiment by Mau-

jean and Descoubes.^{24,27} Wing, Lea, and Lamb²¹ have reported $n^1,^3F_3$ splittings in $n=7, 10,$ and $11,$ but no purely relativistic fs was measured. No other F -state splittings have been published.

The pattern of fs in helium and the Breit-Bethe theory will be discussed in Sec. II. The microwave-optical method will be reviewed in Sec. III, and the apparatus will be described in Sec. IV. The experimental results will be presented and discussed in Secs. V and VI.

II. NATURE OF FINE STRUCTURE IN HIGH SINGLY EXCITED STATES OF HELIUM

A. Survey of helium fine structure

The fine structure in HeI can be considered in two categories: electrostatic and relativistic. The electrostatic splittings displace the energies of the configurations $1snl$ from the corresponding Bohr level $E_n = -hcR/n^2$ to an extent that depends on the orbital angular momentum l . The displacement decreases nearly an order of magnitude for each increase of l by one unit. A further splitting occurs between singlet and triplet terms of the same configuration (e.g., between n^1D and n^3D) with triplets lying below singlets.³³ Except for n^1P states, all terms lie *below* the corresponding Bohr level. In spectroscopic work the term energies are often described by substitution of an effective quantum number, $n^* = n - \delta_l$, in the Bohr formula.^{34,35} Empirically it is found that the quantum defect δ_l varies slowly with n and approaches a definite limiting value as $n \rightarrow \infty$.

In general terms, the origins of the electrostatic splittings are the incomplete screening of the nucleus by the $1s$ electron, resulting in a dependence of term energy on the degree of penetration of the inner electron orbital by the outer; the exchange interaction between the two electrons; and the polarization and distortion of the $1s$ orbital by the excited electron.¹² The average displacement of a configuration $1snl$ from the Bohr level is given by the sum of screening and polarization effects, while the singlet-triplet term splittings result from opposite signs of the exchange interaction in singlet and triplet terms. Approximate resonance frequencies for the electric-dipole transitions $n^{2S+1}L - n^{2S'+1}L'$ can be obtained from optical spectroscopic measurements³¹ or fitted quantum defects.³⁵ Theoretical predictions have resulted from calculations by Pekeris,³⁶ Deutsch,³⁷ Temkin and Silver,³⁸ Chang and Poe,¹² and others.

Relativistic fs interactions further split and displace the terms. In addition, small mass polarization, nuclear motion, and radiative corrections have been studied for $n=2$ to 5 .^{36,39} For the present analysis it is sufficient to consider only the

dominant effects, which are the spin-orbit and spin-spin interactions. These split each triplet term into three fs levels having total angular momenta $J=L+1, L,$ and $L-1,$ while the singlet term has $J=L$. To first order both interactions vanish in singlet terms. The spin-orbit interaction has nonzero matrix elements that connect singlet and triplet levels having the same J and same L . As a result, the two $J=L$ eigenstates in each nL configuration become superpositions of the singlet and triplet $J=L$ basis states and their energies exhibit a mutual repulsion. When the electrostatic singlet-triplet differences are as small as the relativistic interactions, which is true for $L \geq 3,$ the singlet-triplet mixing becomes large,⁹ and a substantial breakdown of Russell-Saunders LS coupling results. The designations "singlet" and "triplet" then only have the meaning that these energy eigenstates would pass continuously into pure singlet and triplet states if the strength of the spin-orbit interaction were reduced to zero. In P and D configurations of helium the electrostatic singlet-triplet intervals are large enough that the degree of repulsion and mixing between corresponding singlet and triplet terms is very slight.^{9,10,40}

In 3D terms of helium the levels form an "inverted triplet," i.e., they are from lowest to highest energy $J=3, 2,$ and 1 . The electrostatic singlet-triplet difference in $7D$ states is³² 13.6 GHz and the relativistic splittings amount to about 100 MHz.

In 3F terms the 3F_3 level is pushed below 3F_4, and the triplet levels from lowest to highest energy are $J=3, 4,$ and 2 . The singlet-triplet difference in $7F$ states is about 150 MHz. The F -state mixing makes possible the observation of "intercombination" resonances, such as $7^1D_2 - 7^3F_3$ reported by Wing *et al.*^{17,20,21} and $7^3D_{2,3} - 7^1F_3$ and $6^1D_2 - 6^3F_3$ reported here. The fs level schemes are indicated for $n=6$ and 7 D and F states of helium in Fig. 1.

B. Breit-Bethe theory

We make use here of the Breit-Bethe (BB) theory of helium relativistic fine structure,⁴ because although it oversimplifies the problem it does provide a frame of reference for the discussion. Furthermore, the assumptions of the theory become more reasonable as l and therefore n increase, and the fs can be calculated easily with fair accuracy. These assumptions are that (a) $r_1 \ll r_2$ where $r_i (i=1, 2)$ are the radial coordinates of the $1s$ and nl electrons; (b) consequently, $r_{12} = |\vec{r}_1 - \vec{r}_2|$ may be replaced by r_2 ; (c) the screening of the nucleus by the inner electron is complete, therefore that the wave function of the outer elec-

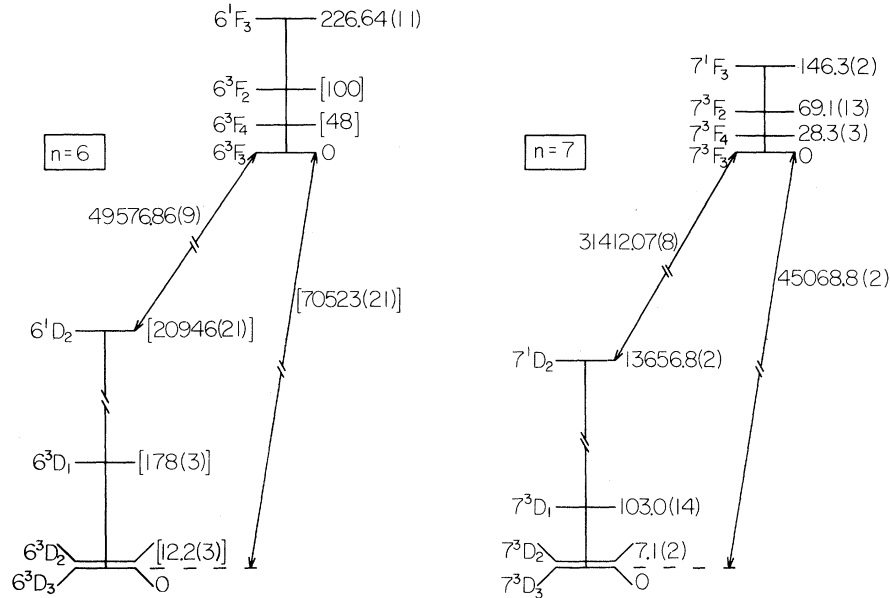


FIG. 1. Fine structure of ${}^4\text{He}$ $n=6$ and $7D$ and F states. The numbers in parentheses are the one-standard-deviation uncertainties in the last digits of the quoted value. Values given in square brackets are taken from Refs. 24, 28, and 32, except as follows: The $6^3D_3-6^3F_3$ interval is the sum of the 6^1D_2 separation in Ref. 32 and the $6^1D_2-6^3F_3$ interval measured in our experiment; and the positions of the 6^3F_2 and 6^3F_4 levels were interpolated by removing the estimated singlet-triplet repulsion from the $n=7$ data, scaling the level energies by a factor $(\frac{7}{6})^3$, and finally applying the estimated singlet-triplet repulsion in $n=6$. These estimates are given in the text. All other values given are results of the present work.

tron is approximately hydrogenic with nuclear charge $Z_{\text{eff}} = Z - 1$; and (d) *unsymmetrized* product wave functions may be used. The terms H_3 (spin-orbit interactions) and H_5 (spin-spin interactions) of the Breit Hamiltonian⁴ then take simple forms for the calculation of matrix elements diagonal in n and L . Following the approach of Bethe,⁴ but retaining the two electron-spin operators separately,³² the singlet-triplet coupling may be included in the theory. The matrix elements can be calculated by angular-momentum algebra⁴¹ and are given in Table I.

The fs level spacings are found by including the exchange energies $\pm K$ in the diagonal matrix elements and solving the secular determinant for a given configuration $1snl$. The ratio of the large and small relativistic fs intervals in 3D terms, neglecting the off-diagonal matrix element of H_3 , is $\nu_{12}/\nu_{23} = 14$, and is independent of n . Here, $h\nu_{JJ'}$ denotes the energy difference between levels J and J' . An exact diagonalization of the matrix shows that the singlet and triplet states having $J=L$ are further shifted up and down, respectively, by an amount $(\delta^2 + G^2)^{1/2} - \delta$, where G is the off-diagonal matrix element and 2δ is the singlet-triplet spacing when G is neglected:

$$2\delta = 2K + (2Rc)(\frac{1}{4}\alpha^2)\langle(a_0/r_2)^3\rangle. \quad (1)$$

Here α is the fine-structure constant and a_0 is the Bohr radius. The second term in Eq. (1) and G are obtained from Table I. Several authors^{8,42,43} have defined a "mixing coefficient" Ω , which measures the relative admixture of the singlet basis function $|S\rangle$ in the wave function $|{}^3L_{J=L}\rangle$. In our notation,

$$\Omega = \frac{\langle S | {}^3L_{J=L} \rangle}{\langle T | {}^3L_{J=L} \rangle} = \frac{-G/\delta}{1 + [1 + (G/\delta)^2]^{1/2}}. \quad (2)$$

Here, $|T\rangle$ is the pure-triplet basis function.

TABLE I. Nonzero matrix elements of the Breit operators H_3 and H_5 in the Breit-Bethe approximation. The matrix elements are to be multiplied by $(2Rc)(\alpha^2/4)\langle(a_0/r_2)^3\rangle$ and are given in Hz. The quantity $\langle(a_0/r_2)^3\rangle$ is obtained from hydrogenic wave functions and equals $2/[n^3(2L+1)(L+1)L]$. R is the Rydberg for helium (cm^{-1}), c the speed of light, α the fine-structure constant, and a_0 the Bohr radius.

S	S'	J	J'	$(H_3)_{SS'JJ'}/h$	$(H_5)_{SS'JJ'}/h$
0	0	L	L	0	0
1	1	$L+1$	$L+1$	$-L$	$2L/(2L+3)$
1	1	L	L	1	-2
1	1	$L-1$	$L-1$	$L+1$	$(2L+2)/(2L-1)$
1	0	L	L	$-3[L(L+1)]^{1/2}$	0

III. MICROWAVE-OPTICAL METHOD

The experiment is based on the microwave-optical technique described by Lamb and Sanders,¹⁸ which is suitable for measuring the fine structure of short-lived atomic states. Atoms are excited by electron bombardment and irradiated simultaneously with a rf that is resonant with an allowed fs transition. The intensity of a spontaneous decay from one of the excited states involved in the fs transition is monitored. When the rf is brought into resonance, the relative populations of the participating fs states are altered and a change is noted in the intensity of the fluorescence. The "signal" (intensity change due to the rf field) is

$$S(\omega) = - (f_a - f_b) \left(\frac{\gamma_a}{\gamma_a} - \frac{\gamma_b}{\gamma_b} \right) \frac{\frac{1}{4}(\gamma_a + \gamma_b) |V|^2}{(\omega - \omega_0)^2 + \frac{1}{4}(\gamma_a + \gamma_b)^2 + (\gamma_a + \gamma_b)^2 |V|^2 / 4\gamma_a\gamma_b} \quad (3)$$

Here, f_β ($\beta = a, b$) are the branching ratios for decay of states β at the wavelength being monitored, γ_β are the excitation rates due to electron bombardment, and γ_β are the effective decay rates due to spontaneous emission and other relaxation mechanisms; $|V|^2 = |\langle a | \mathcal{V} | b \rangle|^2$ is the squared matrix element of the rf perturbation connecting states a and b . The energy difference between the fine-structure states is $\hbar\omega_0 = (E_a - E_b)$, and ω is the angular frequency of the applied microwave field. This line-shape formula applies to a two-level problem, as would be encountered if all degeneracies were lifted, e.g., by the Zeeman effect in a magnetic field.

In the present work no magnetic field is applied. Therefore a fs level J is $(2J+1)$ -fold degenerate. In the absence of perturbations other than the oscillating rf electric field, the axis of quantization is most conveniently taken along the direction of this field, since in this case a selection rule $\Delta M_J = 0$ holds. The resonance between states of angular momenta J_a and J_b therefore consists of $2J_{\min} + 1$ superposed two-level resonances [where $J_{\min} = \min(J_a, J_b)$] all having the same center frequency. From Eq. (3) the two-level resonance

$$S_0 = \frac{\hbar\gamma_a\gamma_b}{2\pi\alpha a_0^2} \left[(2J' + 1)(2J + 1) \begin{pmatrix} J' & 1 & J \\ -M & 0 & M \end{pmatrix} \begin{Bmatrix} L + 1 & J' \\ J & L \end{Bmatrix} S \right]^2 \left(\frac{3}{2}n \right)^2 [n^2 - (L + 1)^2] (L + 1) \quad (4)$$

The radial matrix elements have been obtained using hydrogenic wave functions,⁴ and the $3j$ and $6j$ symbols⁴¹ describe the LS coupling. The resonance connects state $a = |nSLJM\rangle$ to state $b = |nS(L+1)J'M\rangle$. Selection rules $\Delta M = 0$, $\Delta S = 0$, $\Delta L = 1$ and $\Delta J = 0, 1$ are built into the expression. The intercombination resonances are observable because, as mentioned above, the $F(J=3)$ states are actually mixtures of pure singlet and triplet basis states. Since the F states are substantially mixed, nearly the same power is required for $6^1D_2 - 6^3F_3$ as for $6^1D_2 - 6^1F_3$; likewise for the pairs $(7^3D_3 - 7^1F_3)$, $(7^3D_3 - 7^3F_3)$ and $(7^3D_2 - 7^1F_3)$, $(7^3D_2 - 7^3F_3)$.

The resonances are excited by transverse elec-

tric (TE) waves in a shorted section of rectangular wave guide. At the frequencies used in this work the region of excited and radiating atoms overlaps at least two nodes and antinodes in the standing-wave pattern present in the guide. Averaged over the excitation volume, the optimum perturbation is obtained with a forward power

$$W = \frac{1}{4}ABS_0 [1 - (\lambda_0/\lambda_c)^2]^{1/2}, \quad (5)$$

where A and B are the inner dimensions of the guide. Here, λ_c is the cutoff wavelength of the guide in the mode of propagation and λ_0 is the free-space wavelength of the rf. As an illustration, assuming radiative lifetimes $\tau(7^3D) = 145$ nsec and⁴⁵ $\tau(7^3F) = 339$ nsec, the optimum forward power in

a shorted X -band wave guide to drive the $M=\pm 3$ components of the resonance $7^3D_3 - 7^3F_4$ at 45.095 GHz should be 4.2 μW . The power required for the other components is for $M=\pm 2$, 2.4 μW ; $M=\pm 1$, 2.0 μW ; and $M=0$, 1.8 μW . Such small power levels were easily obtained from a harmonic-generation source,⁴⁶ greatly simplifying the requirements for the microwave system. At optimum power the width of the Lorentzian represented in (3) is $\sqrt{2}(\gamma_a + \gamma_b)/2\pi$. This is 2.2 MHz for $7^3D - 7F$ resonances and 2.8 MHz for the $6^1D - 6F$ resonances.

Resonances involving the 7^3D states were seen by monitoring the $7^3D - 2^3P$ decay at 3705 Å. The 4144-Å line from the $6^1D - 2^1P$ decay was monitored for 6^1D resonances. Wing and Lamb¹⁴ used the 4009-Å decay $7^1D - 2^1P$ for detecting the $7^1D - 7F$ resonances.

IV. APPARATUS

The apparatus used has largely been described elsewhere.^{20,47} Helium gas was admitted to an evacuated section of X -band rectangular wave guide maintained at a pressure about 10^{-3} Torr. It was bombarded by an electron beam passing through the narrow faces of the wave guide. Light from the fluorescence of excited states passed out of the wave guide through holes drilled in one of the wider faces and was detected by a blue-sensitive EMI 9635QB photomultiplier. Wavelength selection was provided by an $f/3.5$ Jarrell-Ash $\frac{1}{4}$ -m monochromator or by a dielectric interference filter. The efficiency for light collection was increased by using an internally aluminized ellipsoidal light pipe between the wave guide and the filter or monochromator.

Rf power was coupled into the wave guide from a microwave system based on an OKI 24V11 22–26 GHz 600-mW klystron. The microwave frequency was phase-lock stabilized by a Dymec 2650A oscillator synchronizer with an external Hewlett-Packard P932A wave-guide mixer. The low-frequency reference signal was provided by a Fluke 6160A

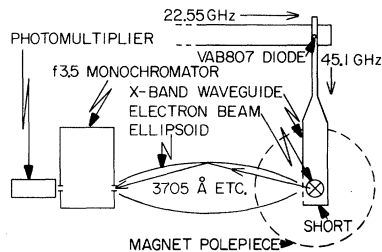


FIG. 2. Apparatus, not to scale. Typical operating conditions are given in Sec. IV.

frequency synthesizer operating at about 130 MHz whose output was tripled and amplified to provide 2 V rms in 50 Ω at 390 MHz. This was mixed with 50 mW sampled from the klystron to produce a beat signal at 30 MHz which was fed to the oscillator synchronizer through a 40-dB i.f. preamplifier. The balance of the phase-locked klystron output at 22–26 GHz was fed into a homemade cross-guide harmonic generator⁴⁶ which used a standard Varian VAB807N10 microwave diode. When the tunable shorts in the ends of the X -band (inside dimensions 22.9 \times 10.2 mm) and R -band (7.1 \times 3.6 mm) wave guides (coupled together through the diode) were adjusted and suitable dc bias was applied to the diode, a pure output at the second-harmonic 44–52 GHz was obtained (Fig. 3). The dc bias on the diode provided both a convenient control of the second-harmonic output level and a means for amplitude modulation. In operation the level was regulated by a feedback circuit, which compared the output of a crystal-diode detector with a reference voltage. The square wave that drove the reference channel of a Princeton Applied Research JB-4 lock-in amplifier was applied to the leveler circuit to “bias off” the harmonic generator (Fig. 3). An on/off ratio greater than 30 dB was obtained in this way.

The electron gun in the X -band resonance module was adjusted to the bombarding energy (30–150 eV) most efficient for exciting the states under study. Bombarding currents were generally varied from run to run to reveal changes in the resonance center or width that might result from space charge or the ambient density of other excited or ionized species. The helium pressure in the mod-

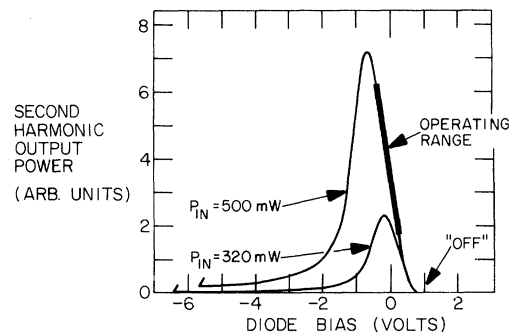


FIG. 3. Second-harmonic output as a function of dc bias applied to the Varian VAB807N10 silicon varactor diode. Positive bias corresponds to forward conduction. Input frequency 25.135 GHz. Second-harmonic output at 50.270 GHz. Maximum conversion efficiency at $P_{IN}=500$ mW is -37 dB. Modulation and power leveling were accomplished by adjusting the bias within the indicated operating range. The microwave power was chopped “off” by applying 1-V forward bias.

ule was controlled by a leak valve from a helium pressure tank, and the system was continuously pumped by a Welch 3102A turbomolecular pump. The pressure was monitored by an ionization gauge.

Single-photon pulses from the photomultiplier were amplified and fed to a discriminator, and their rate was monitored by a General Radio 1142A frequency meter. The FM output of the frequency meter was fed directly to the signal input of the lock-in amplifier tuned to the 43-Hz rate of the reference square wave that was used to modulate the harmonic generator output. The lock-in output was integrated for 100-sec intervals with a Hewlett-Packard 2401C integrating digital voltmeter. The integrated signal and synthesizer frequency were punched on paper tape.

The photomultiplier pulse processing scheme outlined above gave a signal-to-noise ratio approximately twice as great as did analog processing by eliminating the randomness of the photomultiplier pulse heights as a source of noise.

At a pressure 7×10^{-3} Torr and a bombarding current $500 \mu\text{A}$ at 120 V, the count rate from the $7^3D - 2^3P$ 3705-Å line was about 20 kHz.

The resonance module lies between the 30.5-cm poles of a Varian electromagnet because earlier experiments on this apparatus used large magnetic fields to tune the atomic levels into resonance. However, in this work the magnetic field was nulled to less than 100 mG. The residual field was monitored with a Bell 640 gaussmeter.

V. RESULTS

A. $n=6$ resonances

Eighteen scans were made for each of the transitions $6^1D_2 - 6^1F_3$ and $6^1D_2 - 6^3F_3$ near 49.5 GHz. All combinations of bombarding currents 50, 100- and $250\text{-}\mu\text{A}$, helium pressures (0.7, 1.5, and 3.7×10^{-3} Torr), and rf powers approximately 3 and $6 \mu\text{W}$ were used. The electron-bombarding energy was 120 eV. Measurements were distributed across the linewidth at approximately 1.1 MHz intervals. The data were fitted with a Lorentzian line shape in a multiparameter nonlinear least-squares program. The 18 fitted centers and widths for each of the transitions were then analyzed to extract any dependence upon pressure, bombarding current or rf power. The centers were extrapolated to "zero conditions" but the coefficients of rf power and pressure shifts were only marginally significant. No dependence on current was detected. The largest center shifts were 0.08 MHz for $6^1D_2 - 6^1F_3$ and 0.24 MHz for $6^1D_2 - 6^3F_3$. The only significant broadening was that due to micro-

wave power, as expected from Eq. (3). The power broadening was analyzed on the basis of a single-Lorentzian model without the complications described in Sec. III. The extrapolated "natural" linewidths $(\gamma_a + \gamma_b)/2\pi$ were found to be 2.8 ± 0.6 and 3.7 ± 0.6 MHz for the two transitions, respectively. The sum of 6^1D and $6F$ radiative widths expected from the lifetime calculations of Gabriel and Heddie⁴⁵ is about 2.0 MHz. The contributions of Doppler broadening and Zeeman splitting from the residual magnetic field are negligible. There is apparently some additional source of line broadening, which may, moreover, be different for the 6^1F_3 and 6^3F_3 states. The final line-center results are given in Table II. The errors quoted are one standard deviation obtained from the variance-covariance matrix of the least-squares parameters.⁴⁸

B. $n=7$ resonances

The $7^3D - 7F$ resonances near 45 GHz were difficult to locate, but after some searching all eight resonances conforming to $\Delta J=0, \pm 1$ were found. They were considerably weaker than the $6^1D - 6F$ resonances because the 7^3D population is distributed among several fs sublevels, because the excitation cross sections are smaller and possibly because of near cancellation in the factor $r_a/\gamma_a - r_b/\gamma_b$ in Eq. (3). This precluded the extensive study of pressure, current, and rf-power-dependent shifts that was possible in $n=6$. Most of the resonances were measured under conditions of relatively high pressure (7×10^{-3} Torr), bombarding current ($500 \mu\text{A}$), and bombarding voltage (120 V).

The polarity of the resonances correspond to the greater population being in the $7F$ states rather than 7^3D . Because it seemed odd that resonances involving *triplets* should be strongest under conditions more favorable for exciting *singlet* states (i.e., bombarding energies near the peak of singlet cross section), the resonances were later sought at a low bombarding voltage of 40 V. In this case the resonances appeared with opposite polarity (greater population in 7^3D) and only at low helium pressures ($<1.5 \times 10^{-3}$ Torr) (Fig. 4). A possible explanation is that the excitation of triplets at high voltage and pressure was achieved through direct excitation of 7^1P state near the peak of its cross section followed by collisional transfer of excitation into $7F$ states, according to the process studied by several other workers.⁴⁹ Collisional-transfer excitation of the $7F$ states is evidently more effective at the higher energies and pressures than population of 7^3D by direct electron-bombardment excitation, cascade from higher F states, or multiplicity changing collisional trans-

TABLE II. 6^1D_2 - $6F$ intervals.

Designation	Fine-structure interval (MHz) ^a	Other results (MHz) ^b
$6^1D_2-^1F_3$	$49\,803.50 \pm 0.08$	$49\,000^c$ (T) $48\,900^d$ (T, E) $49\,000^e$ (E)
$6^1D_2-^3F_3$	$49\,576.86 \pm 0.09$	$48\,778^c$ (T)
$6^1F_3-^3F_3$	226.64 ± 0.11	222.4^c (T)

^a Present work. Our own measurements throughout the paper are quoted with uncertainties equal to one standard deviation.

^b T = theoretical, E = experimental.

^c Reference 12.

^d Seaton's quantum-defect fit to spectroscopic data for 6^1D and Deutsch polarization theory for $6F$ mean (Refs. 35 and 37).

^e Optical data, $6F$ sublevels not resolved (Ref. 31).

fer from directly excited 7^1P states. At the lower pressures, direct excitation is more likely than collisional transfer. The combination of low voltage and low pressure then favors a greater population of 7^3D than $7F$ states.

The $7^3D_3-7^3F_4$ and $7^3D_1-7^3F_2$ transitions were studied in both modes of excitation. It was found that the latter resonances shifted to lower frequencies at low voltage and pressure, by 2.3 and 1.5 MHz, respectively. The reason for this shift is at present not fully understood, but we believe it to be due to space-charge effects at the low voltages used for direct excitation of the triplets. For this reason only the resonance centers mea-

sured at high voltage and pressure were used to extract the fs splittings, with the exception of the transitions $7^3D_2-7^3F_2$ and $7^3D_3-7^3F_2$, which were measured only at low voltage.

The fitted-center frequencies were averaged for each transition, and the standard deviations of the mean-center frequencies were calculated. These center frequencies and standard deviations were used, together with the two transition frequencies measured by Wing and Lamb²⁰ (see Table III), in a weighted linear least-squares program that extracted all the fs splittings in the $7D$ and $7F$ states. The results are given in Table IV and are reproduced in Fig. 1. After the splittings were determined, the 7^3F_2 level was corrected upward 1.9 ± 1.0 MHz because of the downward shift that was doubtless present in the $7^3D_{2,3}-7^3F_2$ measurements. The 7^3D_1 level was also corrected upward 1.9 ± 1.0 MHz because it can be seen only through its transition to 7^3F_2 . The uncertainties of these two states are therefore correlated.

Since a $\Delta M_J = 0$ selection rule probably inheres

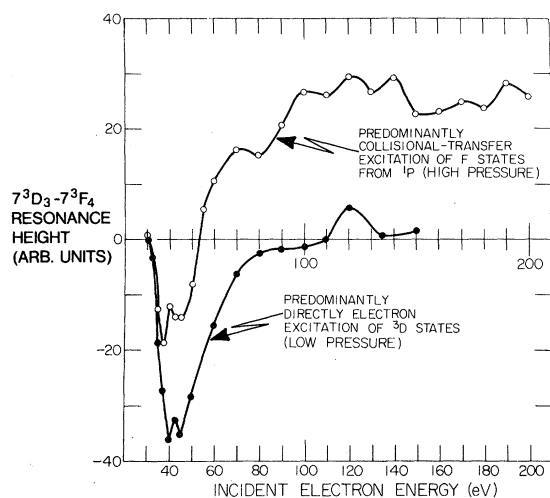


FIG. 4. Resonance height as a function of bombarding energy for low (1.1×10^{-3} Torr) and high (6.5×10^{-3} Torr) pressures. The appearance of the inverted resonance between triplet levels at energies above 80 eV and higher pressures is taken as an indication that in these conditions the 3F states were being populated primarily through collisional excitation transfer.

TABLE III. Frequencies of $7D$ - $7F$ fine-structure resonances used to obtain level splittings.

Transition	Frequency (MHz)	Parametrization
$7^3D_1-7^3F_2$	$45\,034.904 \pm 0.184$	$S-D2+F2$
$7^3D_2-7^3F_3$	$45\,061.530 \pm 0.130$	$S-D1$
$7^3D_3-7^3F_3$	$45\,068.702 \pm 0.477$	S
$7^3D_3-7^3F_4$	$45\,097.078 \pm 0.115$	$S+F1$
$7^3D_2-7^3F_2$	$45\,130.166 \pm 0.402^a$	$S-D1+F2$
$7^3D_3-7^3F_2$	$45\,136.142 \pm 0.177^a$	$S+F2$
$7^3D_2-7^1F_3$	$45\,208.027 \pm 0.070$	$S-D1+F3$
$7^3D_3-7^1F_3$	$45\,215.093 \pm 0.078$	$S+F3$
$7^1D_2-7^1F_3$	$31\,558.260 \pm 0.100^b$	$S-D3+F3$
$7^1D_2-7^3F_3$	$31\,412.070 \pm 0.080^b$	$S-D3$

^a Measured at low voltage and pressure. See text.

^b Wing and Lamb (Ref. 20).

for the microwave transitions seen here, for small magnetic fields the Zeeman splittings should have a magnitude $\Delta\nu_{ab}(M_j) = \mu_0 B M_j (g_a - g_b)/h$. The largest difference of Lande g factors for any of the transitions observed is $\frac{2}{3}$, for the $7^3D_3 - 7^3F_2$ combination. The upper limit of Zeeman splittings in a magnetic field of $B_{\max} = 100$ mG is therefore 0.19 MHz. Unresolved Zeeman splittings of this magnitude, if present, should be symmetrical about the zero-field line centers and therefore would cause no error in the results.

In addition, the Doppler effect should produce a slight symmetrical broadening in the microwave resonances. However, since the atomic Doppler shifts for helium at room temperature are much smaller than the natural linewidths of these resonances, the Doppler width adds to the natural line-

width quadratically, contributing only 1% in the present case.

VI. DISCUSSION

Tables II and IV show that in every case the precision obtained with the microwave-optical method exceeds that obtained by other techniques and that there are substantial discrepancies among the previous results. The calculations by Chang and Poe¹² using Brueckner-Goldstone perturbation theory are quite accurate for the electrostatic D - F intervals and for the singlet-triplet splittings. The calculations of Parish and Mires⁸ are in poor agreement with experiment (for a possible explanation see Ref. 12). The Breit-Bethe theory in 7^3D gives a value D_2 only 6% high but the interval

TABLE IV. Fine-structure intervals in $7D$ and $7F$ states obtained from a weighted linear least-squares fit of the frequencies in Table III. The 7^3F_2 and 7^3D_1 levels have been corrected upward by 1.9 MHz and their uncertainties enlarged (see text). Results of other workers are shown.

Designation	Parameter	Interval (MHz) ^a	Other results (MHz) ^b
$7^3D_3 - 7^3D_2$	D_1	7.1 ± 0.2	6.15 ^c (T)
			7.3 \pm 0.3 ^d (E)
$7^3D_3 - 7^3D_1$	D_2	103.0 ± 1.4	12.3 ^e (T)
			92 \pm 15 ^f (E)
			109.4 ^c (T)
			112 \pm 3 ^g (T, E)
$7^3D_3 - 7^1D_2$	D_3	$13\,656.8 \pm 0.2$	120 ^e (T)
			170 \pm 19 ^h (T, E)
			13\,561 ⁱ (T)
$7^3F_3 - 7^3F_4$	F_1	28.3 ± 0.3	13\,648 \pm 28 ^j (E)
			14\,700 ^k (E)
$7^3F_3 - 7^3F_2$	F_2	69.1 ± 1.3	6.1 ^l (T)
			26 ^m (T)
$7^3F_3 - 7^1F_3$	F_3	146.3 ± 0.2	54.7 ^l (T)
			73 ^m (T)
$7^3D_3 - 7^3F_3$	S	$45\,068.8 \pm 0.2$	143.1 ⁱ (T)
			146.19 \pm 0.13 ⁿ (E)
			44\,484 ⁱ (T)
			44\,700 ^o (T, E)
			46\,200 \pm 600 ^k (E)

^a Present work.

^b T = theoretical, E = experimental.

^c Breit-Bethe theory, see text.

^d Level crossing (Refs. 24 and 27).

^e Reference 8.

^f Beam foil (Ref. 23).

^g Level crossing, scaled by factor $(\frac{6}{7})^3$ from measurement in $n = 6$ (Ref. 28).

^h Level crossing, scaled by factor $(\frac{6}{7})^3$ from measurement in $n = 6$ (Ref. 27).

ⁱ Reference 12.

^j Singlet-triplet anticrossing (Ref. 32), corrected to refer to the 7^3D_3 state rather than the center of gravity of the 7^3D_J fine-structure components.

^k Optical data (Ref. 31).

^l Reference 8.

^m Calculated using method of Araki (Refs. 5 and 20).

ⁿ Microwave optical (Ref. 20).

^o Quantum defects for 7^3D and polarization theory for $7F$ (Refs. 35 and 37).

$7^3F_2 - 7^3F_4$ is predicted to be 19% too great. Neither of these should be affected by the singlet-triplet interaction since $J \neq L$. The reason for the poorer agreement in 7^3F may be the close proximity of the $7G$ state whose effects are neglected, whereas such a perturbation in 7^3D due to the $7F$ states should be about an order of magnitude smaller.

Miller *et al.*³² have compared their measurements of the strength of the singlet-triplet-mixing interaction with the Breit-Bethe theory in $n = (6-8)D$ states. Their quantity Q corresponds to $[L(2L+1)]^{-1/2}$ times the off-diagonal matrix element of H_3 in Table I. If we use calculated lifetimes⁴⁵ instead of the (probably anomalous⁵⁰) lifetime measurements by Descoubes²⁷ that were used by Miller *et al.* in the interpretation of the anticrossing linewidths, we find that the measurements of Miller *et al.* and the Breit-Bethe values agree within 5%.

In view of the moderately good agreement of the Breit-Bethe theory with experiment, it is possible to estimate the amount by which the 7^3D_2 state is depressed in energy through its coupling with the 7^1D_2 state. The Breit-Bethe matrix element between these states is 125.11 MHz (see Table I), while the "unperturbed" separation is approximately the measured singlet-triplet difference $D3 - D1 = 13\,649.7$ MHz. From matrix diagonalization we find that the 7^3D_2 is shifted downward to its observed position by 1.15 MHz. The same analysis in the $7F$ and $6F$ states shows that the depression of 7^3F_3 by 7^1F_3 is approximately 36 MHz and of 6^3F_3 by 6^1F_3 is approximately 61 MHz.

The singlet-triplet mixing coefficients Ω defined in Eq. (2) also result from the diagonalization, in which we use the observed singlet-triplet intervals and the Breit-Bethe matrix elements. The results

TABLE V. Singlet-triplet mixing coefficients Ω estimated from the measured fs intervals and the Breit-Bethe theory. Results of other workers are shown.

State	Ω^a	Other results
7^3D_2	0.00917	0.005 50 ^b 0.0029 ^c
6^3F_3	0.604	0.395 ^b 0.2509 ^c
7^3F_3	0.574	0.363 ^b 0.2263 ^c

^a Present work.

^b Reference 9. These authors calculated the exchange integrals only in first order. The entire discrepancy between their results and ours is, to the present level of accuracy, traceable to this source.

^c Reference 8.

are shown in Table V.

The fitting formula given by Wing *et al.*²¹ for predicting the frequencies of $^1D_2 - ^1,^3F_3$ resonances was used in the present experiment and correctly predicted the $n=6$ transition frequencies within 10 MHz. The formula can be improved on the basis of the present results. Chang⁵¹ has shown that the singlet-triplet splittings should follow a scaling law with respect to n as follows:

$$\Delta T_{n,l} = \sum_{k=0}^l \frac{a_{k,l}}{n^{2k+3}} \quad (6)$$

for states of orbital angular momentum l . In the same spirit, the formula of Wing *et al.* was revised and the microwave-optical resonance data for $n=6, 7, 10,$ and 11 were used to fit a formula of the type

$$\nu_n = A/n^3 + B/n^5 + C/n^7. \quad (7)$$

The coefficients $A, B,$ and C are given in Table VI.

In an early paper on helium fine structure, Breit¹ pointed out that because of the near cancellation of certain quantities it is more appropriate to compare the spin-orbit and spin-spin interactions separately with experiment than to compare the predicted and measured fs intervals or interval ratios as is often done. Inglis⁶ has simplified the calculations of Breit^{1,2} and Araki⁵ and has written the fine-structure separations for a general triplet state in helium in terms of parameters C and d , which measure the strengths of the spin-orbit and spin-spin interactions, respectively. The analysis neglects the singlet-triplet interaction. From our 7^3D data, using the Inglis parametrization, we extract $C = -32.28 \pm 0.45$ MHz and $d = 8.92 \pm 0.17$ MHz when the estimated effect of singlet-triplet repulsion is removed from the data. The Breit-Bethe theory gives $C^{BB} = 34.050$ MHz and $d^{BB} = 9.729$ MHz. The *relative* scale of spin-orbit and spin-spin effects can be compared through the ratio $C/d = 3.62 \pm 0.12$ (experiment) and $C^{BB}/d^{BB} = 3.50$. We therefore find that the greater error of the Breit-Bethe theory in 7^3D is in the *over-all*

TABLE VI. Constants for the fitting formula [Eq. (7)]. With these constants, Eq. (7) fits the observed resonance frequencies in $n=6, 7, 10,$ and 11 within 0.5 MHz.

Transition	A (GHz)	B (GHz)	C (GHz)
$n^1D_2 - n^1F_3$	11 002.08	-8424	-13 650
$n^1D_2 - n^3F_3$	10 948.93	-8287	-13 140

scale of the fine structure, possibly due to the simple way in which $\langle 1/r^2 \rangle$ is calculated, rather than in the relative strengths of the two different relativistic interactions.

ACKNOWLEDGMENT

We would like to thank Professor W. E. Lamb, Jr., for wise counsel throughout the experiment.

- [†]Work supported in part at Yale University by the Air Force Office of Scientific Research under Contract No. F44620-71-C-0042 and at the University of Arizona, Tucson, by the National Science Foundation.
- ¹G. Breit, Phys. Rev. **36**, 383 (1930).
- ²G. Breit, Phys. Rev. **39**, 616 (1932).
- ³W. Heisenberg, Z. Phys. **39**, 499 (1926); Y. Sugiura, Z. Phys. **44**, 190 (1927); J. A. Gaunt, Proc. R. Soc. A **122**, 513 (1929); J. A. Gaunt, Philos. Trans. R. Soc. Lond. **228**, 151 (1929).
- ⁴H. Bethe, *Handbuch der Physik* (Springer, Berlin, 1933), Vol. XXIV; H. Bethe and E. Salpeter, *Quantum Mechanics of One- and Two-Electron Atoms*, (Springer-Verlag, Berlin, 1957).
- ⁵G. Araki, Proc. Phys.-Math. Soc. Jpn. **19**, 128 (1937); G. Araki and S. Huzinaga, Prog. Theor. Phys. **6**, 673 (1951); G. Araki, Phys. Rev. **101**, 1410 (1956).
- ⁶D. Inglis, Phys. Rev. **61**, 297 (1942).
- ⁷R. M. St. John and R. G. Fowler, Phys. Rev. **122**, 1813 (1961).
- ⁸R. M. Parish, Ph.D. thesis (Texas Tech University, Lubbock, Texas, 1970) (unpublished); R. M. Parish and R. W. Mires, Phys. Rev. A **4**, 2145 (1971).
- ⁹R. K. L. van den Eynde, Th. Niemyer, and G. Wiebes, FOM-Instituut voor Atoom-en Molecuulfysica Report No. 31.249 (Amsterdam, 1971) (unpublished); R. K. van den Eynde, G. Wiebes, and Th. Niemyer, Physica (Utr.) **59**, 401 (1972).
- ¹⁰B. Schiff, Y. Accad, and C. L. Pekeris, Phys. Rev. A **8**, 2272 (1973).
- ¹¹A. F. J. van Raan and H. G. M. Heideman, J. Phys. B **7**, L216 (1974).
- ¹²T. N. Chang and R. T. Poe, Phys. Rev. A **10**, 1981 (1974).
- ¹³W. V. Houston, Phys. Rev. **29**, A794 (1927); Proc. Natl. Acad. Sci. USA **13**, 91 (1927).
- ¹⁴W. E. Lamb, Jr. and T. H. Maiman, Phys. Rev. **105**, 573 (1957).
- ¹⁵A. Kponou, V. W. Hughes, C. E. Johnson, S. A. Lewis, and F. M. J. Pichanick, Phys. Rev. Lett. **26**, 1613 (1971).
- ¹⁶W. H. Wing, D. L. Mader, and W. E. Lamb, Jr., Bull. Am. Phys. Soc. **16**, 531 (1971).
- ¹⁷W. E. Lamb, Jr., D. L. Mader, and W. H. Wing, in *Fundamental and Applied Laser Physics, Proceedings of the Esfahan Symposium*, edited by M. S. Feld, A. Javan, and N. A. Kurnit (Wiley, New York, 1973), pp. 523-538.
- ¹⁸W. E. Lamb, Jr. and T. M. Sanders, Phys. Rev. **119**, 1901 (1960).
- ¹⁹L. R. Wilcox and W. E. Lamb, Jr., Phys. Rev. **119**, 1915 (1960).
- ²⁰W. H. Wing and W. E. Lamb, Jr., Phys. Rev. Lett. **28**, 265 (1972).
- ²¹W. H. Wing, K. R. Lea, and W. E. Lamb, Jr., in *Atomic Physics 3*, edited by S. J. Smith and G. K. Walters (Plenum, New York, 1973), p. 119.
- ²²H. Andrä, Phys. Scr. **9**, 257 (1974).
- ²³H. G. Berry, J. L. Subtil, and M. Carre, J. Phys. (Paris) **23**, 947 (1972); H. G. Berry and J. Subtil, Nucl. Instrum. Methods **110**, 321 (1973).
- ²⁴M. Maujean and J. P. Descoubes, C. R. Acad. Sci. B **264**, 1653 (1967).
- ²⁵R. D. Kaul, J. Opt. Soc. Am. **58**, 429 (1968).
- ²⁶K. Buchhaupt, Z. Naturforsch. **24A**, 1058 (1969).
- ²⁷J. P. Descoubes, in *Physics of the One and Two Electron Atoms*, edited by F. Bopp and H. Kleinpoppen (North-Holland, Amsterdam, 1969), p. 341.
- ²⁸D. Dily and J. P. Descoubes, C. R. Acad. Sci. B **272**, 1182 (1971).
- ²⁹A.-M. Pilon, J. Phys. Radium **15**, 692 (1954); G. Herzberg, Proc. R. Soc. A **248**, 309 (1958).
- ³⁰U. Litzen, Phys. Scr. **2**, 103 (1970).
- ³¹W. C. Martin, J. Phys. Chem. Ref. Data **2**, 257 (1973).
- ³²T. A. Miller, R. S. Freund, T. Foch, T. J. Cook, and B. R. Zegarski, Phys. Rev. A **9**, 2474 (1974); T. A. Miller, R. S. Freund, and B. R. Zegarski, Phys. Rev. A **11**, 753 (1975).
- ³³R. P. Messmer and F. W. Birss, J. Phys. Chem. **75**, 2085 (1969).
- ³⁴J. R. Rydberg, K. Sven. Vetenskapsakad. Handl. **23**, No. 11 (1889); Philos. Mag. **29**, 331 (1890); C. R. Acad. Sci. (Paris) **110**, 394 (1890); Z. Phys. Chem. (Leipzig) **5**, 227 (1890).
- ³⁵M. J. Seaton, Proc. Phys. Soc. Lond. **88**, 815 (1966).
- ³⁶C. L. Pekeris, B. Schiff, and H. Lifson, Phys. Rev. **126**, 1057 (1962); B. Schiff, H. Lifson, C. L. Pekeris, and P. Rabinowitz, Phys. Rev. **140**, A1104 (1965); Y. Accad, C. L. Pekeris, and B. Schiff, Phys. Rev. A **4**, 516 (1971).
- ³⁷C. Deutsch, Phys. Rev. A **2**, 43 (1970).
- ³⁸A. Temkin and H. Silver, Phys. Rev. A **10**, 1439 (1974).
- ³⁹M. Douglas and N. M. Kroll, Ann. Phys. (N.Y.) **82**, 89 (1974).
- ⁴⁰L. Hambro, Phys. Rev. A **5**, 2027 (1972); L. Hambro, Phys. Rev. A **6**, 865 (1972); L. Hambro, Phys. Rev. A **7**, 479 (1973).
- ⁴¹A. R. Edmonds, *Angular Momentum in Quantum Mechanics* (Princeton U.P., Princeton, N. J., 1960).
- ⁴²G. Araki, M. Ohta, and K. Mano, Phys. Rev. **116**, 651 (1959).
- ⁴³G. W. F. Drake, Phys. Rev. **181**, 23 (1969).
- ⁴⁴I. C. Percival and M. J. Seaton, Philos. Trans. R. Soc. Lond. A **251**, 113 (1958).
- ⁴⁵A. H. Gabriel and D. W. O. Heddle, Proc. R. Soc. A **258**, 124 (1960).
- ⁴⁶W. Gordy, W. V. Smith, and R. F. Trambarulo, *Micro-wave Spectroscopy* (Dover, New York, 1966), pp. 48-53.
- ⁴⁷R. R. Jacobs, K. R. Lea, and W. E. Lamb, Jr., Phys. Rev. A **3**, 884 (1971); D. L. Mader, M. Leventhal, and W. E. Lamb, Jr., Phys. Rev. A **6**, 1832 (1971); S. L. Kaufman, W. E. Lamb, Jr., K. R. Lea, and M. Leven-

thal, Phys. Rev. A 4, 2128 (1971).

⁴⁸W. C. Hamilton, *Statistics in Physical Science* (Ronald, New York, 1964).

⁴⁹B. L. Moiseiwitsch and S. J. Smith, Rev. Mod. Phys. 40, 238 (1968). Two examples of more recent work are J. D. Jobe and R. M. St. John [Phys. Rev. A 5, 295 (1972)] and A. F. J. van Raan and J. van Eck [J. Phys. B 7, 2003 (1974)].

⁵⁰A search of the literature on helium-lifetime measurements revealed the following: In 4^1D , 19 out of 20 mea-

surements fell in an interval -13% to $+24\%$ around the theoretical calculation in Ref. 45. In 5^1D , 12 out of 13 measurements (excluding Descoubes, Ref. 27) fell in an interval -22% to $+10\%$ around the theoretical value while Descoubes's value was 33% lower than theory. In 6^1D and 7^1D states, where they are the only available measurements, Descoubes's values fell 50% and 66% lower, respectively, than the theoretical calculation.

⁵¹T. N. Chang, J. Phys. B 7, L108 (1973).